Int. J. Rock Mech. Min. Sci. & Geomech. Abstr. Vol. 18, pp. 487 to 503, 1981
Printed in Great Britain.

0148-9062/81/060487-17$02.00/0

Some Aspects of 'Characterization' Problems in Geomechanics

A. CIVIDINI*
L. JURINA*
G. GIODA*

The paper presents a discussion of some of the aspects of parameter 'characterization' problems (or back analyses) in the field of Geomechanics. In the first part of the paper, inverse *and* direct *procedures are discussed for the solution of characterization problems with reference to linear material behaviour. The direct procedure is then applied to the determination of geometry, material and load parameters, on the basis of the displacements obtained from a hypothetical* in-situ *load test. Finally, the influence of the number of input data (and of the experimental errors affecting them) on the results of characterization problems is discussed.*

INTRODUCTION

Characterization (or system identification or back calculation) problems, in the fields of Structural and Geotechnical Engineering, are strictly related to classical stress analysis problems. In fact, even though their aims are different, they involve the same relevant mechanical quantities and the same governing relations. In order to clarify the differences and the similarities between the two problems, consider first the basic feature of a stress analysis problem.

When a complex Geotechnical or Rock Mechanics problem has to be analyzed, it is often necessary to develop a numerical model (based e.g. on a finite element discretization of the geotechnical medium) 'equivalent' to the physical system. Here the term 'equivalent' means that the answer of the numerical model to defined external actions must be as close as possible to that of the real system to the same actions.

Three fundamental groups of data, describing the real system, are necessary to set up the numerical model:

(i) data on the system geometry, defining the shape of the geotechnical medium to be analysed, of the zones formed by different materials and of the zones where external loads or constraints are applied;

(ii) data on the materials, which define the laws describing the material behaviour and the values of the material parameters;

(iii) data defining the load distributions.

Having developed the numerical model, the solution of the stress analysis problem consists of:

(iv) the complete description of the displacement field (as well as of the pore pressure distribution for problems involving two-phase media);

(v) the strain and effective stress distributions throughout the medium.

In order to define the characterization problem, consider a geotechnical work after its completion (or a large scale *in-situ* test) and assume that a set of measurements of some quantities belonging to sets iv or v is performed (e.g. displacements or stress components at some locations of the medium). In addition, assume that some of the data of either sets i, ii or iii are unknown or only partially defined: for instance: the shape of a cavity or of an inclusion; the distribution of the interaction pressures between soil and a retaining structure; the values of the mechanical parameters describing the behaviour of some part of the geotechnical medium; etc.

On these bases, the characterization (or model calibration) problem [1,2] can be stated as follows: define the values of the unknown quantities (belonging to sets i, ii or iii) that adopted in the stress analysis of the geotechnical system lead to results (belonging to sets iv and v) as close as possible to the available experimental data.

Depending on the nature of the unknown parameters, characterization problems can be subdivided into three categories, concerning the determination of:

(a) geometry characteristics;
(b) material parameters;
(c) loads.

* Department of Structural Engineering, Technical University (Politecnico) of Milan, Piazza Leonardo da Vinci, 32, 20133 Milano, Italy.

In principle, any characterization problem can be solved in one of two ways, which will be referred to in what follows as *inverse* and *direct* approaches.

The *inverse* approach is based on a formulation opposite to that adopted for the stress analysis. In fact, the equations governing the stress analysis problem are re-written in such a way that some of the quantities of either groups i, ii or iii (corresponding to the parameters to be identified) appear in the sets of unknowns, while some of the quantities of groups iv or v (corresponding to the experimental measurements) appear in the set of data. Since the number of available *in-situ* measurements usually exceeds the number of unknown parameters, the final system contains more equations than unknowns and the solution has to be based on a suitable optimization procedure.

The *direct* approach adopts the same numerical model used for stress analysis, within the framework of an iterative procedure; hence, no formulation of the inverse problem is required. The iterative (minimization) procedure allows for correcting the trial values of the unknown parameters adopted in the stress analysis until the discrepancy between experimental data and the corresponding numerical results is minimized.

In this paper some aspects of the use of computational characterization procedures in the field of Geotechnical and Rock Engineering are discussed. Firstly, in order to clarify the differences between the two solution approaches, an inverse and a direct procedures are briefly described with reference to determination of elastic parameters. While the inverse approach is limited to this type of problem only, the direct one has more general validity and is suitable for the solution of a range of characterization problems.

In order to achieve some insight into the performance of the direct procedure, its application to characterization problems type (a), (b) and (c) is discussed in the second part of the paper, with reference to a simple illustrative example.

The third part of the paper discusses the influence of the number (*quantity*) of the available measurements and of the experimental error affecting them (i.e. their *quality*) on the results of the analysis. It is shown that, for a given problem, it is possible to define the relationship existing between quality and quantity of the input data and quality (e.g. standard deviation) of the computed results. This information could be useful in order to "design" an *in-situ* test, i.e. in order to define the minimum number and precision of the *in-situ* measurements necessary to obtain values of the unknown parameters with a pre-defined confidence limit.

Notation: Bold face capital letters denote matrices. Bold face lower case letters denote column vectors. Superscript T means transpose.

CHARACTERIZATION VIA INVERSE AND DIRECT APPROACHES

In this section inverse and direct approaches for the determination of the average values of elastic parameters of geotechnical systems (problem type *b*) are briefly described. The inverse approach is a modified version of a procedure originally proposed by Kavanagh [3] for structural problems, and subsequently [4] suggested for geotechnical problems, while the direct one is based on *direct search* methods for function minimization [5]. Both of them refer to a compatible finite element discretization of the geotechnical medium.

Inverse formulation

As customary when adopting the finite element method for structural analysis, the stiffness matrix $\mathbf{K}^e$ of the e-th finite element is defined as follows:

$$\mathbf{K}^e = \int_v \mathbf{M}^T \mathbf{D} \mathbf{M} \, dv \tag{1}$$

where $\mathbf{M}$ is the nodal displacement-strain matrix; $\mathbf{D}$ is the elastic constitutive matrix and v is the element volume.

Matrix $\mathbf{D}$ can be expressed as the sum of two terms linearly depending on the bulk B and shear G moduli, respectively:

$$\mathbf{D} = B\mathbf{D}_B + G\mathbf{D}_G \tag{2}$$

By substituting equation (2) into equation (1), the following expression of $\mathbf{K}^e$ is obtained:

$$\mathbf{K}^e = B\mathbf{K}_B^e + G\mathbf{K}_G^e \tag{3}$$

In equation (3), $\mathbf{K}_B^e$ and $\mathbf{K}_G^e$ are matrices representing, respectively, the volumetric and deviatoric stiffnesses of the e-th finite element assuming B and G equal to 1. Analogously, the stiffness matrix $\mathbf{K}$ of the assembled finite element system can be expressed in the following form:

$$\mathbf{K} = \sum_j^m (B_j \mathbf{K}_{Bj} + G_j \mathbf{K}_{Gj}) = \sum_i^{2m} p_i \mathbf{K}_i \tag{4}$$

where the coefficients p_i represent the shear and bulk moduli of the m different materials considered in the numerical model (i.e. the problem unknowns) and $\mathbf{K}_i$ is the stiffness matrix computed by assuming all the material parameters equal to zero, except for $p_i = 1$.

In the following it is assumed that the boundary conditions have been already imposed on each matrix $\mathbf{K}_i$ and, hence, that matrix $\mathbf{K}$ is not singular.

Assuming that n displacement components of points of the real system have been measured in the field, and that these points concide with nodes of the finite element mesh, the nodal force-nodal displacement relationship can be written as follows:

$$\begin{bmatrix} \mathbf{K}_{11} & \mathbf{K}_{12} \\ \mathbf{K}_{21} & \mathbf{K}_{22} \end{bmatrix} \begin{Bmatrix} \mathbf{u}_1^* \\ \mathbf{u}_2 \end{Bmatrix} = \begin{Bmatrix} \mathbf{f}_1 \\ \mathbf{f}_2 \end{Bmatrix} \tag{5}$$

In equation (5), vector $\mathbf{u}_1^*$ contains the measured displacements while the remaining (unknown) ones are grouped in vector $\mathbf{u}_2$.

Since matrix $\mathbf{K}$ is not singular, a static condensation can be performed on equation (5) in order to eliminate the unknown displacement vector $\mathbf{u}_2$. Some algebraic

manipulations lead to:

$$(\mathbf{K}_{11} - \mathbf{Q}\mathbf{K}_{21})\mathbf{u}_1^* = \mathbf{f}_1 - \mathbf{Q}\mathbf{f}_2 \tag{6}$$

where

$$\mathbf{Q} = \mathbf{K}_{12}\mathbf{K}_{22}^{-1} \tag{7}$$

By substituting equation (4) into equation (6) one obtains

$$\sum_1^{2m} p_i \mathbf{r}_i = \mathbf{f}_1 - \mathbf{Q}\mathbf{f}_2 \tag{8}$$

where

$$\mathbf{r}_i = (\mathbf{K}_{11,i} - \mathbf{Q}\mathbf{K}_{21,i})\mathbf{u}_1^* \tag{9}$$

In the above equations, matrices $\mathbf{K}_{11,i}$ and $\mathbf{K}_{21,i}$ are obtained by partitioning matrix $\mathbf{K}_i$ according to $\mathbf{u}_1^*$ and $\mathbf{u}_2$.

Grouping the unknown coefficients p_i in the $2m$-vector $\mathbf{p}$ and grouping vectors $\mathbf{r}_i$ in the $(n \times 2m)$-matrix $\mathbf{R}$,

$$\mathbf{R} = [\mathbf{r}_1\ \mathbf{r}_2 \ldots \mathbf{r}_{2m}] \tag{10}$$

equation (8) can be re-written as

$$\mathbf{R}\mathbf{p} = \mathbf{f}_1 - \mathbf{Q}\mathbf{f}_2 \tag{11}$$

Two points are worth mentioning with reference to equation (11): matrix $\mathbf{K}$ is a function of the unknown parameters $\mathbf{p}$, thus also matrix $\mathbf{Q}$ (through equation 7) and matrix $\mathbf{R}$ (through equations 10 and 9) are functions of vector $\mathbf{p}$. Necessary, but not sufficient, condition for the solution of equation (11) is that the number n of measured displacements be equal to, or greater than, the number $2m$ of unknown parameters.

Assuming $n > 2m$, the solution of the non-linear system (11) can be reached by means of an iterative procedure.

An initial trial vector $\mathbf{p}$ is chosen, on the basis of which matrices $\mathbf{R}$ and $\mathbf{Q}$ are computed. The error ϵ obtained by introducing an arbitrary vector $\mathbf{p}$ in equation (11) (where matrices $\mathbf{R}$ and $\mathbf{Q}$ are now constants) can be defined as follows:

$$\epsilon = (\mathbf{R}\mathbf{p} - \mathbf{f}_1 + \mathbf{Q}\mathbf{f}_2)^T(\mathbf{R}\mathbf{p} - \mathbf{f}_1 + \mathbf{Q}\mathbf{f}_2) \tag{12}$$

By minimizing ϵ with respect to $\mathbf{p}$, in the *least square* sense, the following system is arrived at:

$$\mathbf{R}^T\mathbf{R}\mathbf{p} = \mathbf{R}^T(\mathbf{f}_1 - \mathbf{Q}\mathbf{f}_2) \tag{13}$$

the solution of which leads to a new vector $\mathbf{p}$. Matrices $\mathbf{R}$ and $\mathbf{Q}$ are then recalculated and the iterations are carried on until the difference between the vectors $\mathbf{p}$ at two subsequent steps decreases below a chosen limit.

Direct formulation

The direct approach is based on the minimization of the following error function

$$\epsilon = \left\{\sum_1^n [u_i - u_i^*]^2\right\}^{1/2} \tag{14}$$

and thus represents a least squares reduction of the discrepancy between the n displacements u_i^* measured in the field and the corresponding data, u_i, obtained by the numerical analysis of the geotechnical problem. Since the numerical data u_i depend on the values of the elastic parameters $\mathbf{p}$ assumed in the finite element calculation, the error ϵ is in turn function of these parameters (i.e. $\epsilon = \epsilon(\mathbf{p})$). Thus, the elements of vector $\mathbf{p}$ minimizing ϵ represent the values of the elastic constants which lead to the best description of the behaviour of the real system by means of the chosen numerical model.

The error defined by equation (14) is a highly non-linear function of the material parameters, even when linearly elastic behaviour is assumed. Therefore, the minimization algorithm adopted for the problem solution must be capable to handle general non-linear functions and, since the analytical expression of ϵ cannot be defined, the algorithm must not require the analytical evaluation of the function gradient. Algorithms meeting with the above requirements are known in Mathematical Programming as *direct search methods* [5] (e.g. Simplex, Rosenbrock's, Powell's, etc.). These are iterative procedures which perform the minimization process, in the space of the $2m$ parameters $\mathbf{p}$, solely by successive evaluations of the error function $\epsilon(\mathbf{p})$. Each evaluation requires a stress analysis (e.g. by means of a finite element calculation) of the geotechnical problem on the basis of the trial vector $\mathbf{p}$ for that iteration.

Previous studies on characterization problems of type (b) [4,6] have shown that the inverse approach converges towards the optimal values of the unknown parameters faster than the direct procedure. However, other points have to be considered in order to assess the superiority of one of them. In fact, approaches of the direct type can be based on standard computer programs for function minimization in which the finite element code for stress analysis is introduced as a subroutine. This can be done with negligible modification of the finite element code and with limited programming effort. In addition, the same stress analysis program and error minimization algorithm can be adopted for various characterization problems, merely by considering the displacements $\mathbf{u}$ [equation (14)] functions of the unknown parameters, regardless of their nature. For instance, an application of a direct approach to the determination of shear strength parameters and *in-situ* state of stress in rock masses has been presented in [7].

In contrast to direct methods, inverse approaches require the implementation of *ad hoc* computer programs for the solution of the inverse problem. These programs can be obtained only by substantial modifications of the stress analysis code and by implementing a series of new subroutines for matrix manipulation. As a consequence, the programming effort required by inverse approaches is, in general, larger than that required by direct approaches. Furthermore, every inverse formulation depends on the very nature of the characterization problem, thus a new computer program has to be developed for each type (a, b or c) of analysis.

From these observations it appears that direct approaches might be preferable, especially when the solution of the stress analysis problem can be carried out by standard computer codes in common use. A notable exception is the quadratic programming approach to the determination of yield limits described in [9]. In this case, standard quadratic programming subroutines can be used for solving both the elastic-plastic stress analysis [10] and the characterization problems with minor modifications of the computer code.

In order to accelerate the convergence of direct search algorithms, the following alternative definition of the error function can be adopted.

$$\epsilon = \left\{ \sum_{1}^{n} {}_i \left[u_i(\mathbf{p}') - u_i^* \right]^2 \right\}^{1/2} \tag{15a}$$

where

$$\mathbf{p}' = \frac{1}{\chi} \mathbf{p} \tag{15b}$$

At every iteration the vector of parameters $\mathbf{p}$, defined at the end of the previous step, is divided by a scalar coefficient χ, the value of which is computed by minimizing the error function $\epsilon(\chi)$ defined by equations (15).

The meaning of coefficient χ can be clarified considering that vector $\mathbf{p}$ represents a point P in the space of the elastic parameters and that vector $\mathbf{p}'$, depending on the value of χ, represents a point of the straight line connecting P with the origin O. Thus, χ defines the point of the line Op in which ϵ reaches its minimum.

On the basis of the assumption of linear elastic behaviour, equation (15a) can be re-written as follows:

$$\epsilon = \left\{ \sum_{1}^{n} {}_i \left[\chi \cdot u_i(\mathbf{p}) - u_i^* \right]^2 \right\}^{1/2} \tag{16a}$$

which, by imposing that ϵ be stationary with respect to χ (i.e. $d\epsilon/d\chi = 0$), leads to the following final expression:

$$\chi = \frac{\mathbf{u}(\mathbf{p})^T \mathbf{u}^*}{\mathbf{u}(\mathbf{p})^T \mathbf{u}(\mathbf{p})} \tag{16b}$$

Note that the error function defined by equations (16) can be used only for the determination of elastic parameters, while that defined by equation (14), as previously observed, is applicable to various characterization problems.

In the following sections some examples of characterization analyses are discussed. Their solution is based on the direct search algorithm known as the Simplex method, and on the error function defined by equation (14) or (16) depending on the type of problem. A discussion of the algorithm properties falls outside the limits of the present work. Details can be found in [5,8].

AN ILLUSTRATIVE EXAMPLE OF PARAMETER DETERMINATION

In order to demonstrate some basic aspects of characterization analyses it is convenient to consider a simple illustrative example. To this purpose, the hypothetical *in-situ* load test schematically shown in Fig. 1a is adopted. The problem refers to a weak rock layer, resting on a sound rock bed, which contains an inclusion of softer material and is acted upon by a vertical surface load distribution q.

A numerical model of the real system can be based on the finite element discretization of Fig. 1b. In order to define the characteristics of the real system and, hence, of the numerical model, assume that: (1) the

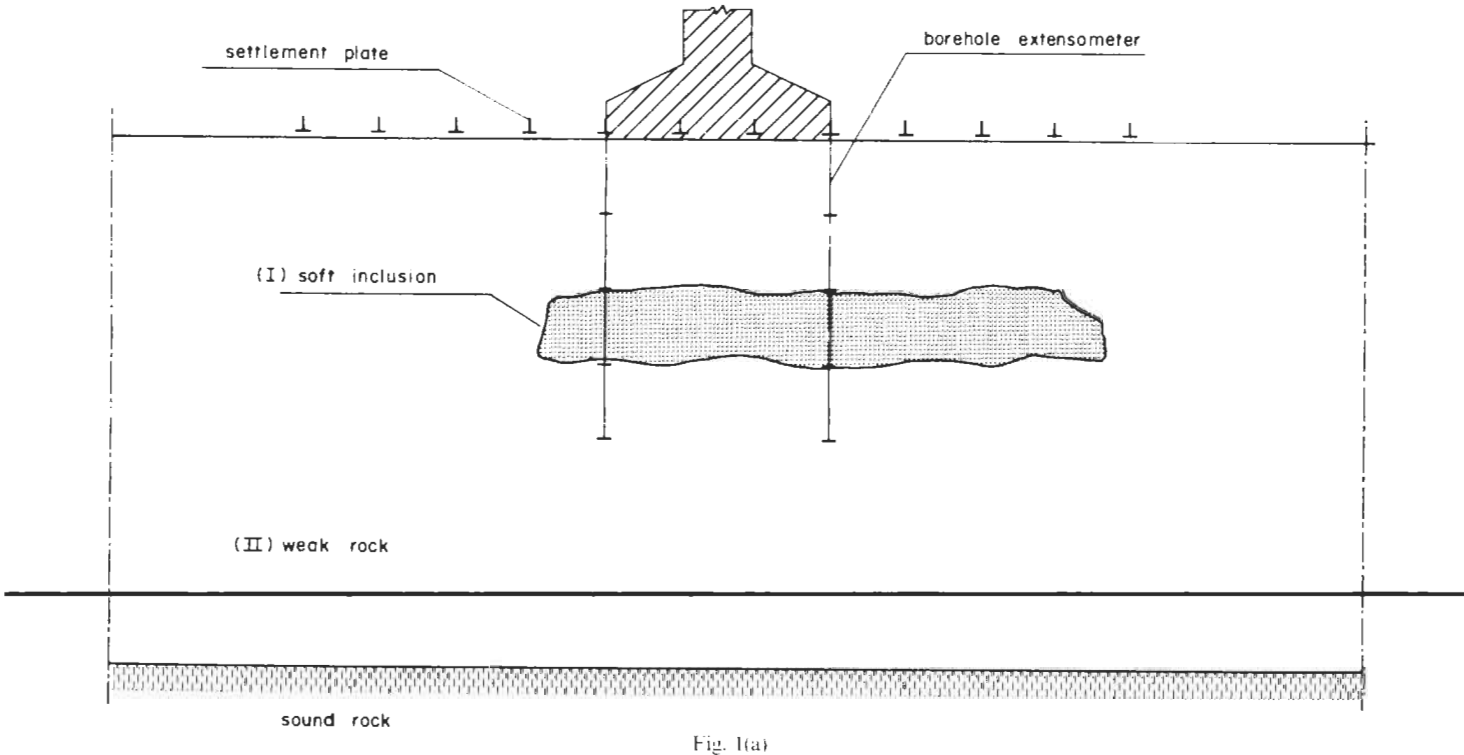

Fig. 1(a)

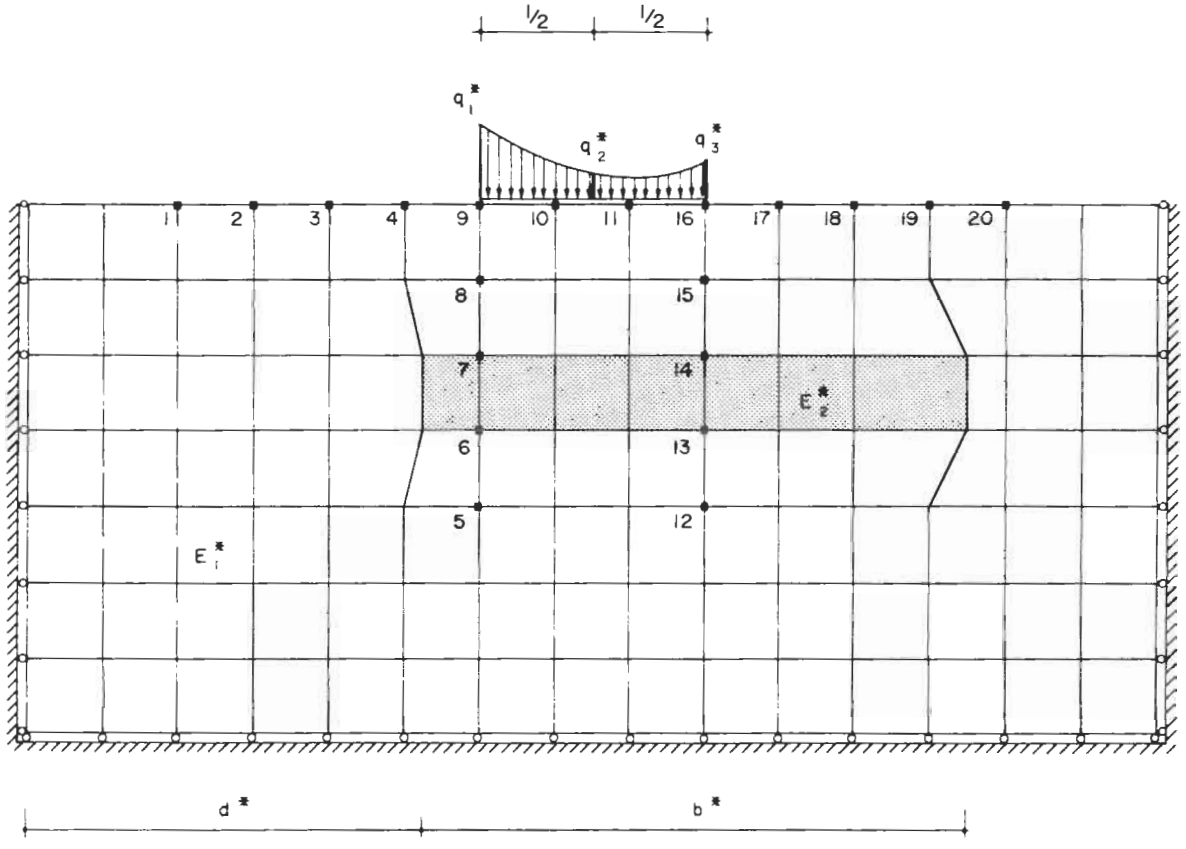

Fig. 1(b)

Fig. 1. Schematic representation (a) of the example adopted for the identification analyses and its finite element discretization (b).

depth and thickness of the lens and the size of the loaded zone are known: (2) the load distribution is parabolic and its resultant R is known: (3) the real rock behaviour can be approximated by the isotropic linear elasticity and the Poisson ratios of zones I and II are known.

Under these assumptions the following additional data are necessary for the complete description of the numerical model: (a) the dimensions h^* and d^*, defining the position and size of the inclusion: (b) the elastic moduli E_1^* and E_2^* of rocks I and II: (c) the values of the parabolic load distribution at two locations, say q_1^* and q_2^*.

If some of the data of either groups (a), (b) or (c) are unknown, their values can be defined by means of a direct characterization analysis, knowing the displacements of some points of the medium caused by the surface load distribution. Note that the above assumptions have been introduced only to limit the number of problem variables, not because of lack of generality of the solution procedure.

A first series of analyses was carried out in order to check the performance of the direct search algorithm and to get some estimate of the computational cost. To this purpose, the 'real' displacements have been generated numerically, by means of a finite element analysis, and the input data of each characterization analysis consist of the vertical displacements of the 20 nodes denoted by black squares in Fig. 1b.

In what follows a star denotes the 'real' values of the parameters to be identified.

The first analysis, based on the minimization of the error function defined by equation (14), has the geometry parameters h and d as free variables, while elastic moduli and loads are known. The results of this analysis are summarized in Fig. 2 where the contour lines of the error function and the optimization path (light solid line) are shown in the h, d plane. Note that the contour lines are shown merely to visualize the shape of the error function; of course this information is not required by the minimization algorithm. A circle and a black dot represent, respectively, the arbitrarily chosen starting point and the 'optimal' point. The feasible region for error minimization is bounded by the d axis (in fact no physical meaning can be associated to negative values of the lens length), by the h axis (i.e. $d > 0$) and by the inclined dashed line, expressing the condition that the total distance $h + d$ must not exceed the length of the discretized zone.

Trial values of h and d are defined at every iteration of the minimization process: the mesh is automatically modified in order to account for the new shape of the lens and the error function is computed by means of the finite element analysis. If a trial point of the optimization path violates one of the constraints, the error for that point is assigned a very high value. This, when direct search methods are used, brings the path back into the feasible region without requiring algorithm

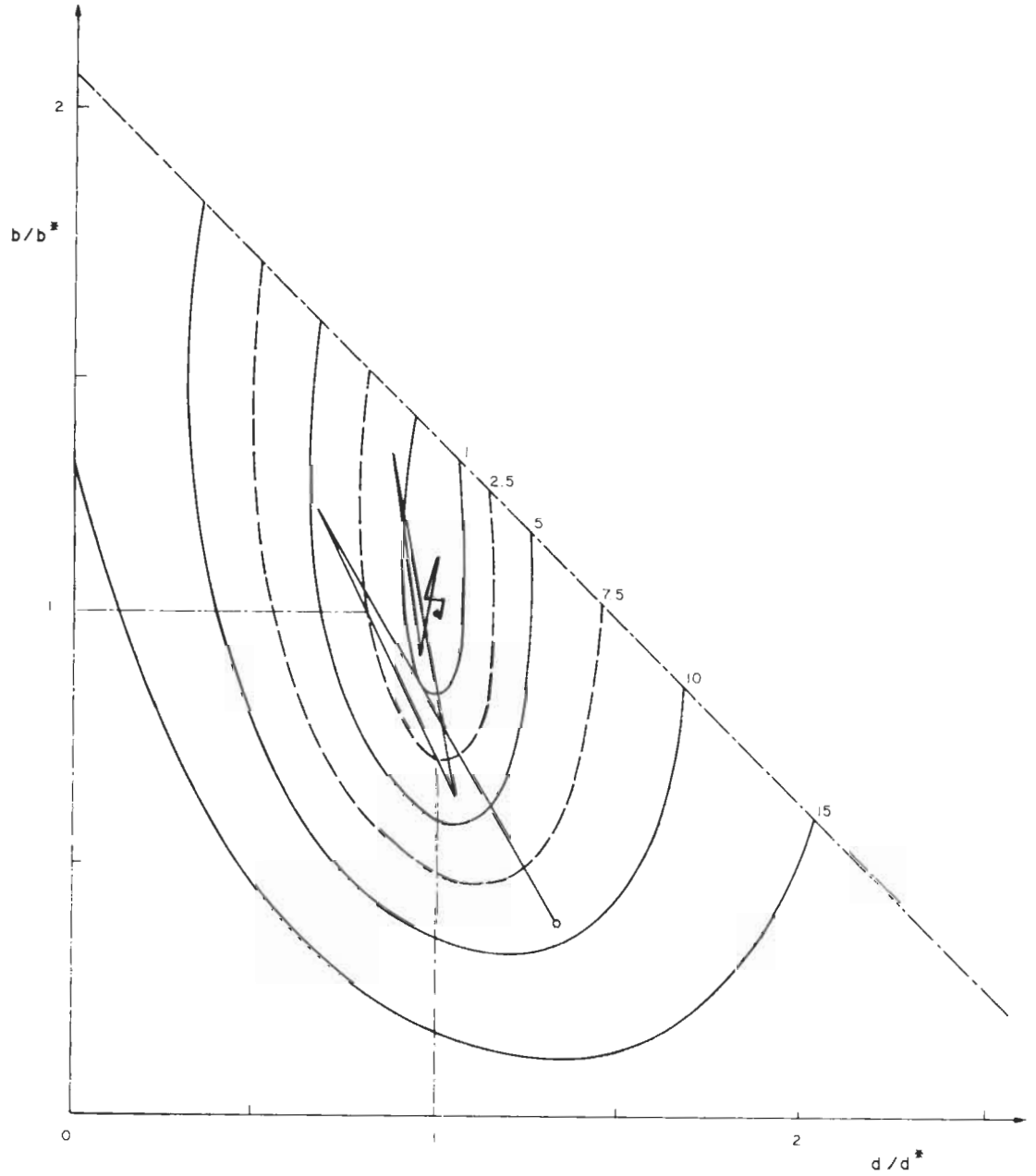

Fig. 2. Error contour lines and optimization path for the characterization of the geometry parameters b and d on the basis of 20 "exact" displacement data (a star denotes the "real" values of the parameters).

modifications or additional computational effort. Note that the constraints represented by the b axis and by the inclined straight line are related to the size of the discretized zone, rather than to the physical nature of the problem. Therefore, if the optimal point falls on one of these boundaries the mesh pattern has to be enlarged, and a new minimization has to be performed, in order to allow for a larger size of the soft inclusion.

The free variables of the second analysis consist of the elastic moduli E_1 and E_2. In this case the calculations can be simplified by adopting the error function defined by equations (16). This is equivalent to assume a radial co-ordinate system r, θ in the E_1 E_2 plane

$$\tan\theta = E_1/E_2; \quad r^2 = E_1^2 + E_2^2 \qquad (17a,b)$$

The value of r which minimizes the error function, for a given value of θ, can be easily computed by means of equation (16b), where $\alpha = 1$ r and the entries E_1 and E_2 of vector $\mathbf{p}$ are defined by equations (17) with $r = 1$. Since the error minimization along the radial co-ordinate is performed analytically, the numerical minimization via direct search algorithm becomes one-dimensional and involves only the angular co-ordinate. The contour lines of the error function and the minimization path for this analysis are shown in Fig. 3. In this case the feasible region for error minimization coincides with the first quadrant (i.e. E_1 and $E_2 > 0$).

Assuming as known data the elastic moduli, the lens geometry and the total load R, the determination of load parameters q_1, q_2 (and q_3) is straightforward and does not require numerical minimization of the error. In fact, because of the assumption of linear elastic be-

haviour, the displacement vector **u** can be expressed in the following form:

$$\mathbf{u}(q_1, q_2, q_3) = \sum_{1}^{3} q_i \mathbf{u}_i \tag{18}$$

where $\mathbf{u}_i$ is the displacement vector for $q_i = 1$ and $q_j = 0$ $(j \neq i)$.

Since the modulus R of the resultant of the parabolic load distribution is known, a linear relationship can be established between q_1, q_2 and q_3. By expressing q_3 as a function of q_1 and q_2, equation (18) can be re-written as follows:

$$\mathbf{u} = \mathbf{u}_0' + q_1\mathbf{u}_1' + q_2\mathbf{u}_2' \tag{19}$$

in which $\mathbf{u}_0'$, $\mathbf{u}_1'$ and $\mathbf{u}_2'$ are suitable linear combinations of $\mathbf{u}_1$, $\mathbf{u}_2$, $\mathbf{u}_3$.

The optimal values of the load parameters can be readily calculated by substituting equation (19) into equation (14) and by imposing that the error function be stationary with respect to q_1 and q_2. Due to its simplicity, the determination of load parameters was not considered.

The third analysis involves both elastic moduli and loads as free variables. Note that this analysis would not be possible without knowing the resultant R of the applied loads. In fact, the same displacement vector **u** (and, hence, the same value of the error function) is obtained if both loads and elastic moduli are multiplied by the same quantity. Thus, the optimal values of the free variables, i.e. the coordinates of the minimum of the error function, cannot be uniquely defined.

Knowing the load resultant, the parameters q_1, q_2, E_1 and E_2 can be identified by adopting a radial co-ordinate system r, θ in the E_1, E_2 plane. The minimization along the angular co-ordinate is based on the direct search algorithm. For every trial value of θ the minimization along the radius is performed analytically, as previously described, in terms of q_1, q_2 and r as free

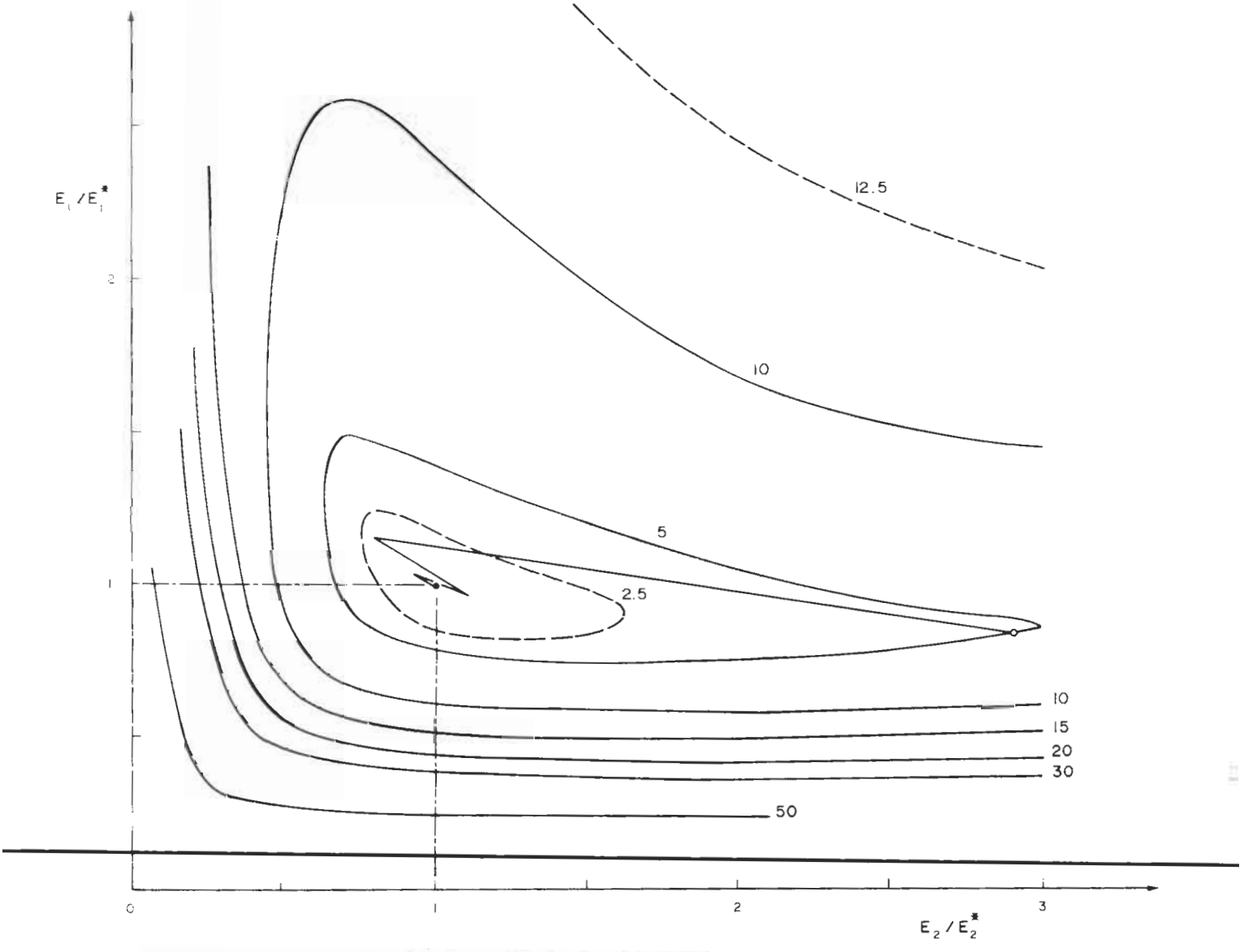

Fig. 3. Error contour lines and optimization path for the characterization of the elastic moduli E_1 and E_2 (other characteristics as in Fig. 2).

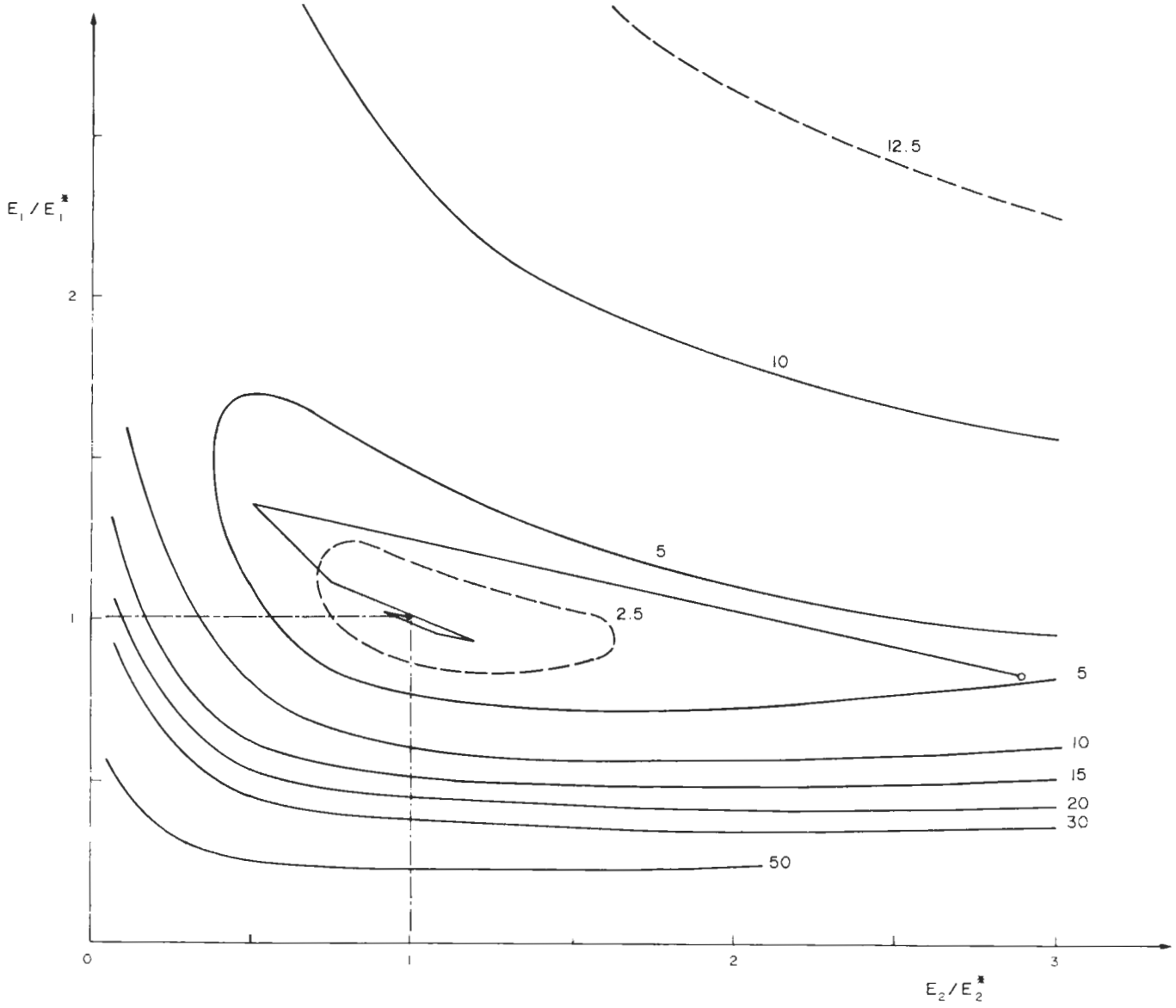

Fig. 4. Error contour lines and optimization path for the characterization of the elastic moduli and load parameters (other characteristics as in Fig. 2).

variables. The results of this analysis are presented in Fig. 4. It can be observed that the error contour lines and the optimization path shown in Fig. 3 (known load distribution) are only slightly different from those of Fig. 4 (load parameters as free variables): from the computational standpoint the costs of the two analyses did not differ appreciably.

Geometry, material and load parameters are, simultaneously, the free variables of the last analysis. Even though six variables are considered, the minimization process can be split into two parts, each one involving three variables only. The minimization in terms of θ (or E_1, E_2, cf. equation 17b), b and d is carried out numerically. For every trial point in the E_1, E_2, b, d space the minimization in terms of r (cf. equation 17b), q_1 and q_2 is performed analytically as previously described. In Fig. 5, the optimization path in the θ, b, d space is shown.

The results of the above analyses show that direct search algorithms (the Simplex method, in the present context) represent a suitable tool for the solution of various kinds of characterization problems involving a limited number of variables. Even though a finite element analysis is required by each error evaluation, the computational effort was rather limited (about 66 CPU sec on a UNIVAC 1100 81 computer, for the solution of the 2 parameter (b, d) analysis).

For all the examples considered, the solution coincided, within the numerical tolerance, with the real values of the free variables. This is due to the fact that a maximum of 6 parameters was to be identified on the basis of 20 'exact' displacement measurements. However, if the number of measurements, and or their accuracy, is reduced, it is likely that the determined parameters would differ substantially from the real ones, or that it would not be possible to carry out the character-

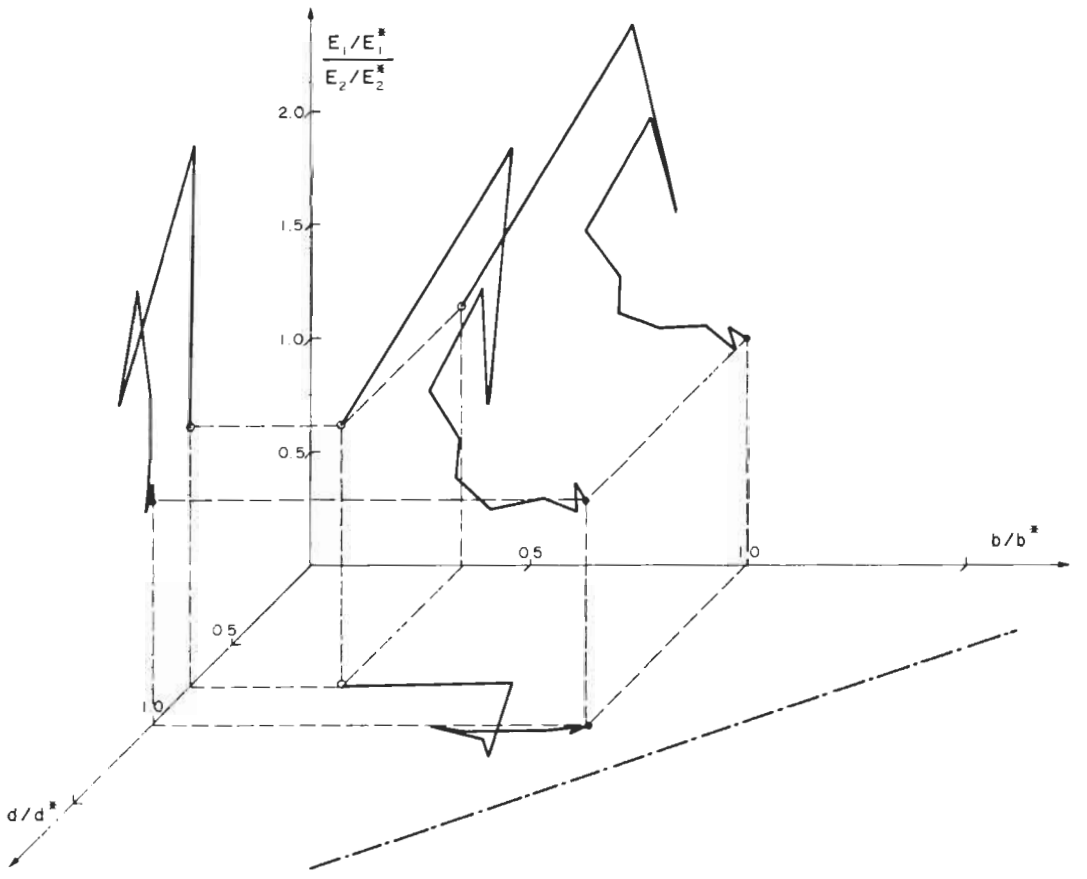

Fig. 5. Optimization path for the characterization of the elastic moduli, geometry parameters and loads (other characteristics as in Fig. 2).

ization analysis because of lack of experimental information. The effect of the number of measurements has been investigated, with reference to a structural engineering problem, in [9].

INFLUENCE OF THE EXPERIMENTAL ERRORS

Any *in-situ* measurement is affected by experimental errors which depend on the nature of the measured quantity, on the instrument adopted, on the field conditions, etc. In order to define the influence of these errors on the results of characterization problems (at least for the example here considered), a series of numerical tests have been performed, each containing $N_t = 1000$ analyses having as input data 10 vertical displacements, defined at points No. 1, 3, 5, 7, 9, 12, 14, 16, 18, 20 of Fig. 1b.

The experimental errors are simulated by generating 1000 sets of 10 numbers each, using 10 independent generators of random numbers with Gaussian probability distribution and zero mean value. The N_t input displacement vectors for the analyses of each test are obtained by adding the error sets to the 'exact' displacement vector, which was obtained numerically as previously described.

The numerical tests are subdivided into groups, each one consisting of three tests related, respectively, to the determination of: (a) geometry parameters b and d; (b) elastic moduli E_1 and E_2; (c) load parameters q_1 and q_2. Each group of three tests is characterized by different approximations of the input data. Since every analysis leads to different optimal values of the free variables, depending on the input data errors, the results of the numerical tests can be suitably represented by means of frequency diagrams (or histograms).

In the graphical representation of the results of tests, the optimal values of the free variables are divided by their 'exact' values (denoted by a star) which, for all the tests performed, coincide with the histogram mean values.

For the first three numerical tests, the results of which are summarized in Figs 6–8, the standard deviation of the error distribution is equal to 1/3 mm. This is equivalent, in engineering terms, to assuming that the *in-situ* measurements are performed by means of instruments having resolution $\delta = \pm 1$ mm. Note that the maximum and minimum 'exact' values of the vertical displacements considered as input data are 12.0 and 0.35 mm, respectively.

The results of the N_t analyses concerning the determination of the lens geometry are summarized in Fig. 6. The histogram in the b, d plane is represented by means of black dots. The dot size depends on the number N of optimal values of the free variables falling in a rec-

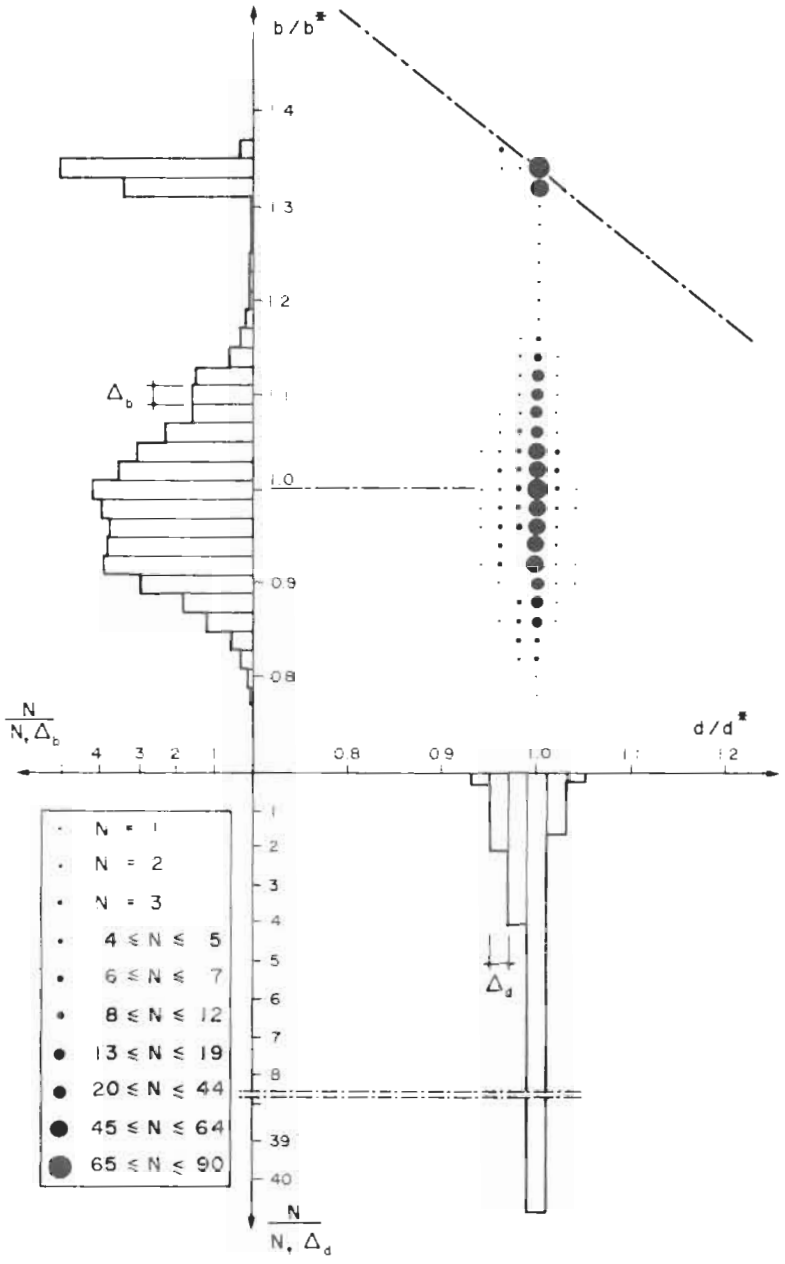

Fig. 6. Histograms of the optimal values of the geometry parameters b and d obtained by $N_s = 1000$ characterization analyses (10 *in situ* measurements; Gaussian error distribution with standard deviation of 1.3 mm).

tangular area $\Delta_b \times \Delta_d$ the center of which coincides with the dot center. The projections of this histogram on the b and d axes are also presented.

The inclined dashed line in the b, d plane represents the constraint of the feasible region whose meaning has been discussed in the previous section.

It can be noted that the optimal values of b are much more dispersed than those of d. This can be explained by considering that the underground measurement points (cf. Fig. 1) are close to the first edge of the inclusion (the position of which is defined by the distance d) and far from the second one (the position of which is defined by the distance b). In addition, the first edge is much closer to the loaded zone than the second one. As a consequence, the gradient of the error function, on which basis the problem is solved (cf. equation 14), is larger with respect to d than the gradient with respect to b (cf. Fig. 2). In turn, the optimal value of d is more stable, with respect to the measurement errors, than the optimal value of b.

The histogram along the b axis presents a peak located on the boundary of the feasible region. This depends on the fact that for some of the error vectors the lens length reaches the limit imposed by the size of the finite element mesh. The peak could be avoided by enlarging the discretized zone. However, this provision has no effect on the dispersion of the optimal values of b, which can only be reduced by modifying the pattern of the measurement points and by increasing their number in the zone close to the second edge of the inclusion.

Because of the influence of the numerical model geo-

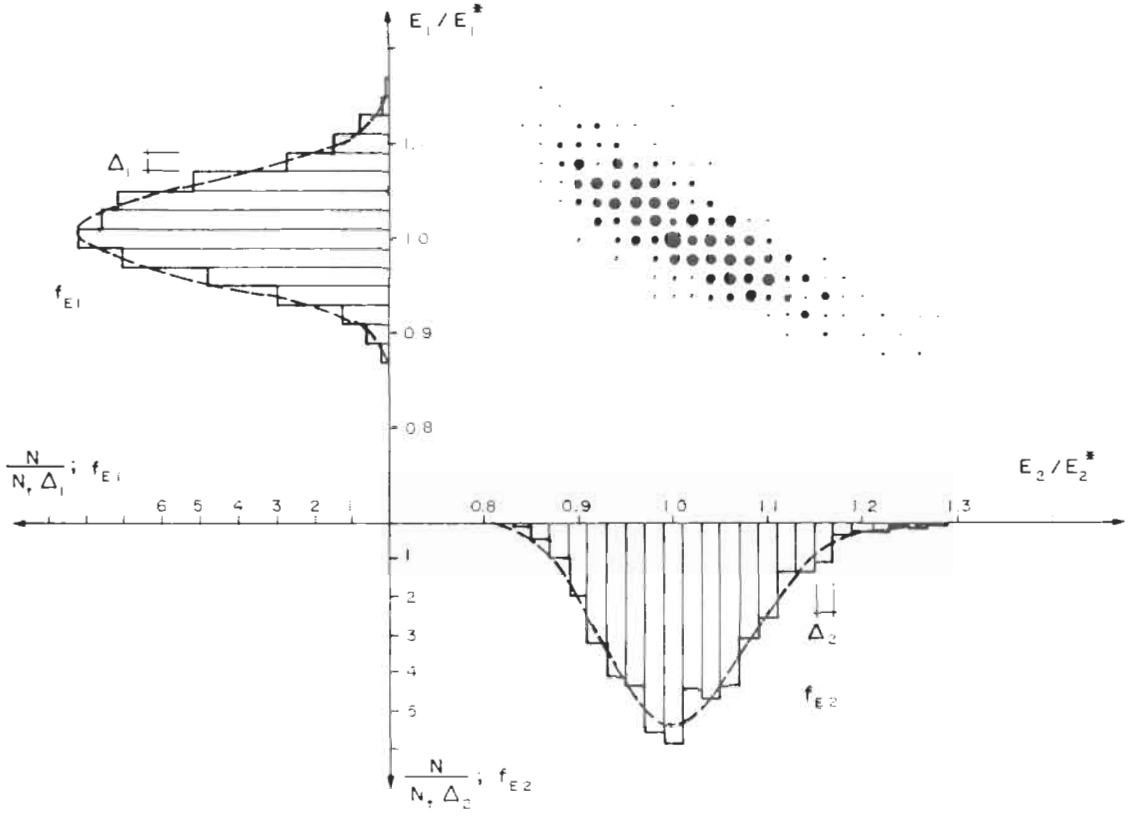

Fig. 7. Histograms of the optimal values of the elastic moduli E_1 and E_2 and the related log-normal probability density functions f_{E1} and f_{E2} (other characteristics as in Fig. 6).

metry on the distribution of the optimal values of b, no attempt was made to interpret the results of analyses by means of some standard probability distribution.

Figure 7 shows the results of the characterization analyses of the elastic moduli E_1 and E_2. The scatter of the optimal values of E_1 (weak rock) is smaller than that of the optimal values of E_2 (soft inclusion). This is due to the fact that most of the discretized zone consists of material having modulus E_1. Thus the determination of this parameter is less affected by the experimental errors than that of E_2, representing the modulus of the smaller zone.

As expected, a certain correlation exists between the distributions of the optimal values of the two moduli. It can be observed that the histograms along the E_1 and E_2 axes are not symmetric with respect to their mean values. In fact, while relatively high moduli can be reached even for relatively small measurement errors, values of the moduli close to zero could be obtained only by assuming very large standard deviation of the error distribution.

An attempt to describe the results of analyses by means of the log-normal probability distribution is presented in Fig. 7. This distribution was chosen merely for its simplicity and for its non-symmetric shape, which is similar to that of the reported histograms. The parameters of the two probability density functions f_{E1} and f_{E1} are computed on the basis of the mean values and standard deviations of the histograms of E_1 and E_2, respectively.

The last series of analyses of the first group concerns the determination of the load parameter q_1 and q_2. Figure 8 reports the histograms of the optimal values of the free variables, and the related Gaussian probability density functions f_{q1} and f_{q2}. For the sake of completeness, the histogram of the optimal values of q_3 (linearly dependent on those of q_1 and q_2) is also shown.

As for the previous case, the correlation exists between the distributions of the optimal values of the free variables, and one of them (q_2) is more dispersed than the other one (q_1). This last effect can be explained by recalling that q_1 and q_2 are values of the distributed load at two different locations and that the measurement points are closer to the first location than to the second one. As a consequence, the influence of q_1 on the measured displacements is larger (and, in turn, its determination in the presence of experimental errors is more accurate) than that of q_2.

Other numerical tests have been carried out assuming resolutions δ for the displacement measurements equal to ± 0.5 mm and to ± 2.0 mm. The results of the tests are summarized in Figs 9 and 10, showing the probability density functions of the optimal values of elastic moduli and load parameters obtained with various values of δ. The results of analyses suggest the following considerations about the determination of different variables on the basis of the same data, in presence of experimental errors: (1) the scatter of the optimal values of 'distributed' parameters (like the elastic moduli) appears smaller than that of 'local' par-

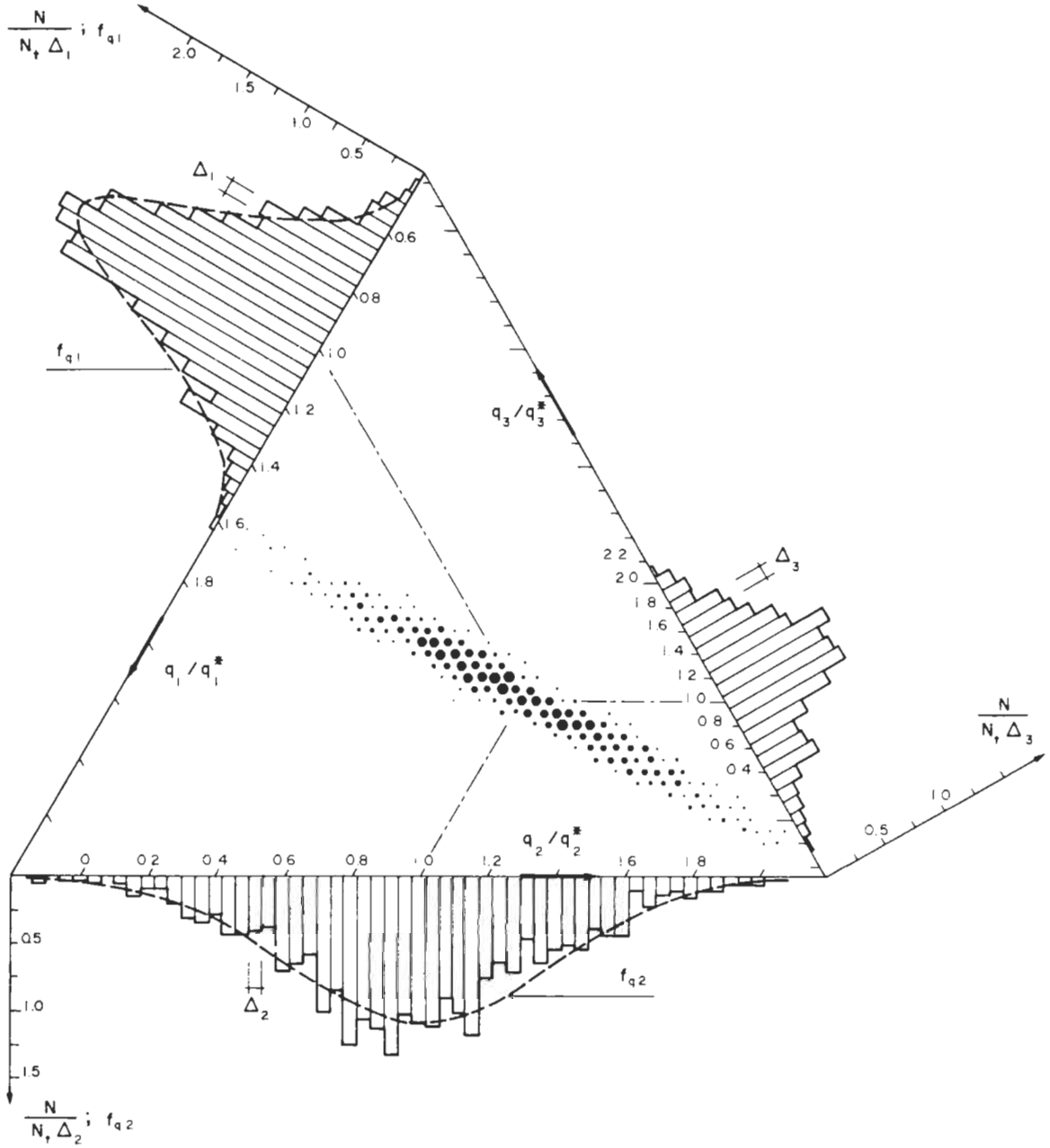

Fig. 8. Histograms of the optimal values of the load parameters q_1, q_2 (and q_3) and the related Gaussian probability density functions f_{q1} and f_{q2} (other characteristics as in Fig. 6).

ameters (like the values of distributed loads at some locations); (2) the scatter of 'distributed' parameters decreases with increasing size of the zone which they are related to (i.e. the dispersion of the elastic modulus of the inclusion is larger than that of the rock surrounding it); (3) the scatter of 'local' parameters increases by increasing the distance between measurements points and the points where parameters are defined.

INFLUENCE OF THE NUMBER OF *IN-SITU* MEASUREMENTS

The successful characterization of a field problem requires, in addition to a sufficient accuracy of the *in-situ* measurements:

(i) a careful selection of the locations for observations;

(ii) a significant level of redundancy in the number of experimental observations.

To assess the effect that the number of measurements has on the scatter of the optimal values of the free variables, some numerical tests based on 20 and 6 measurements have been performed. For the 20-measurement test the settlements of all the points denoted by black squares in Fig. 1b were considered, while for the 6-measurement tests the input data are the settlements of points 3, 7, 9, 14, 16, 18.

Several 6- and 20-measurement tests and some additional 10-measurement tests, have been carried out assuming various accuracies δ of the input data. The

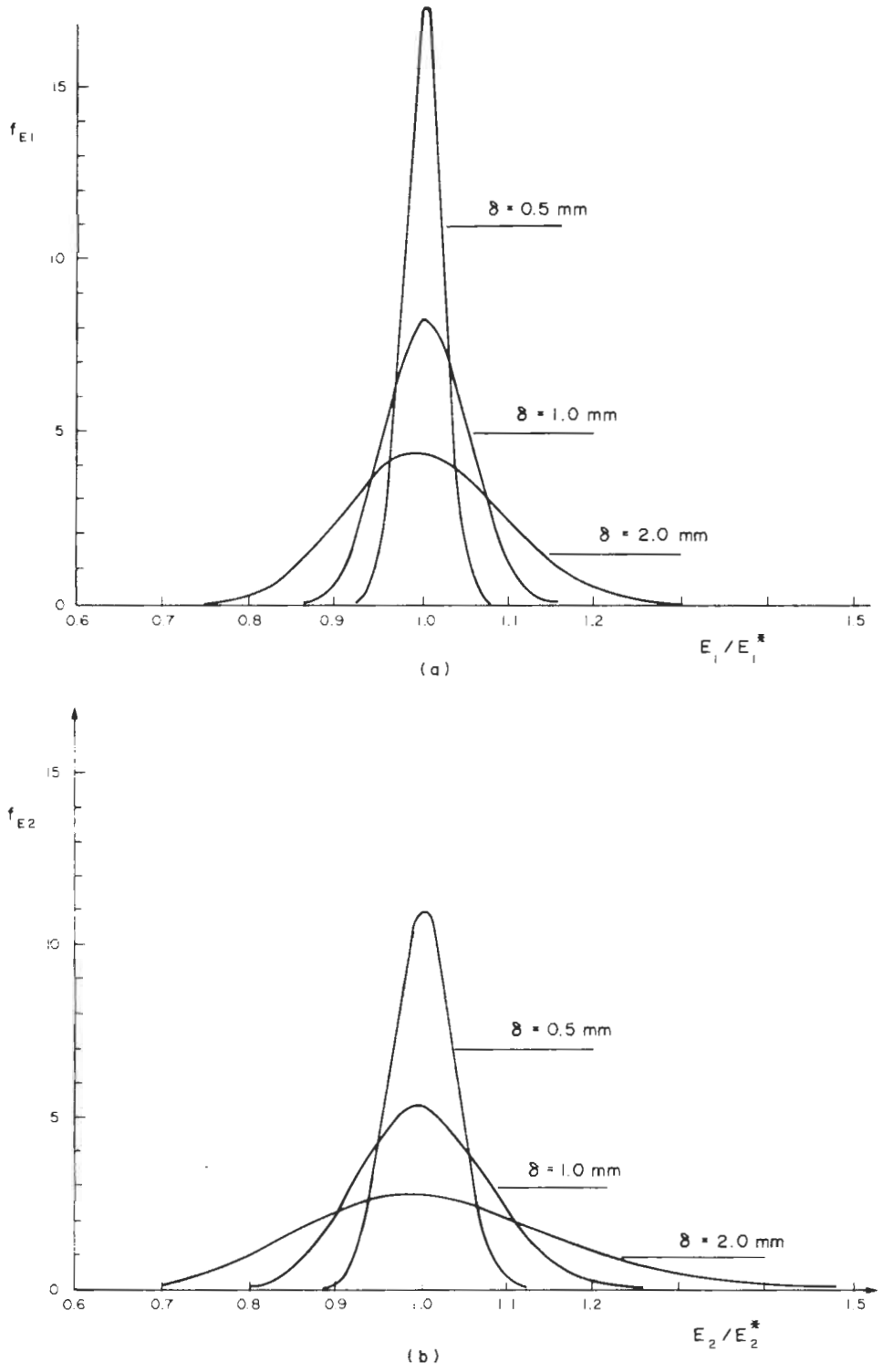

Fig. 9. Log-normal probability density functions of the optimal values of the elastic moduli E_1 and E_2 for various approximations δ of the input displacements.

results of analyses are reported in compact form in Figs 11–13, through the plots of the non-dimensional standard deviations of the optimal values of the free variables vs δ.

The following definition is adopted for the non-dimensional standard deviation of a generic variable x:

$$s_x = \left\{ \frac{1}{(N_t - 1)} \sum_{i}^{N_t} \left(\frac{x_i - x^*}{x^*} \right)^2 \right\}^{1/2} \tag{20}$$

where N_t is the number of data and x^* is their mean value.

The diagrams of Fig. 11b, related to the determination of the geometry parameter h, are clearly influenced by the constraint on the length of the inclusion imposed by the mesh size. In fact, since the size of the lens cannot exceed that of the discretized zone, increasing the approximation δ of the input data (i.e. decreasing the displacement accuracy) the standard

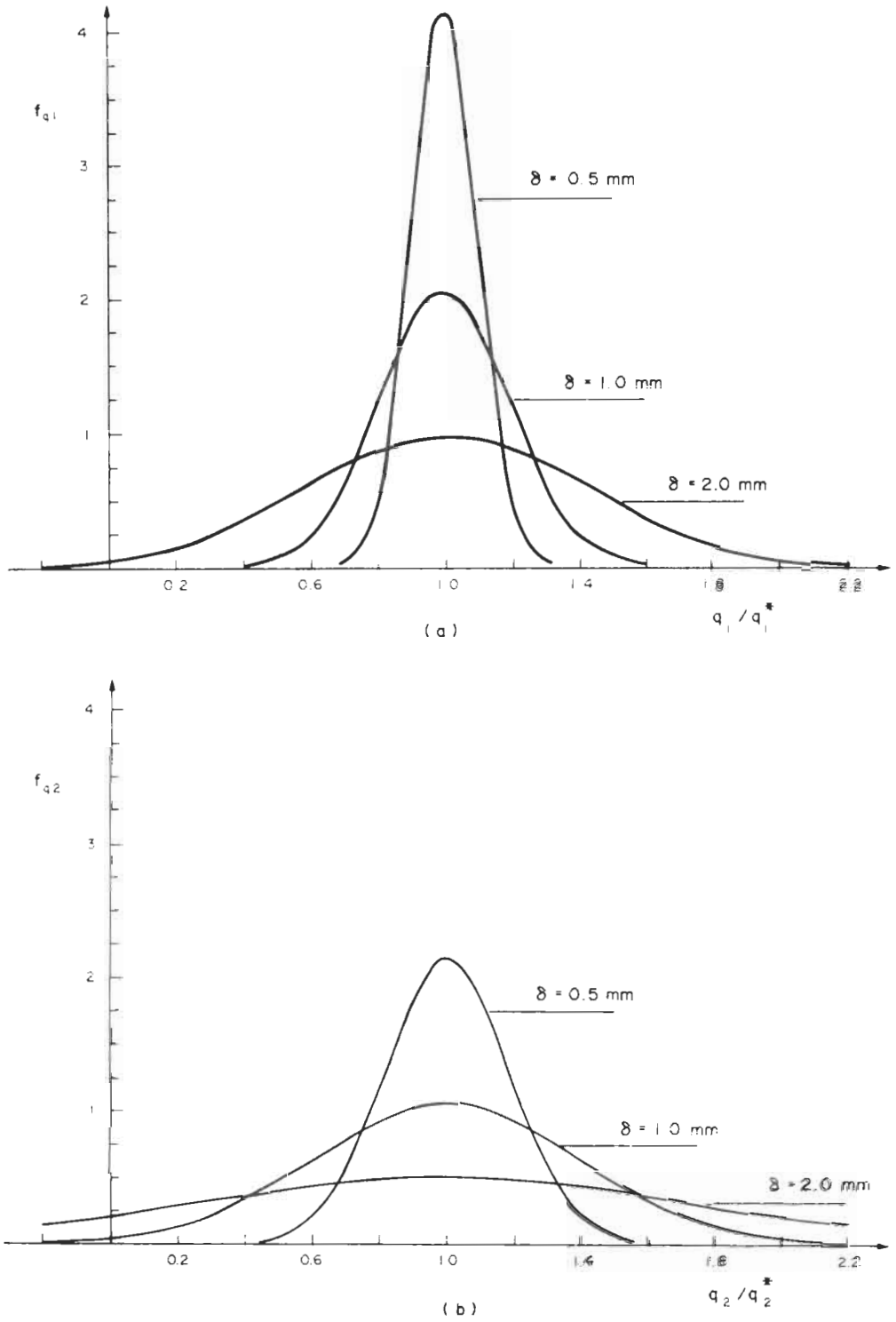

Fig. 10. Gaussian probability density functions of the optimal values of the load parameters q_1 and q_2 for various approximations δ of the input displacements.

deviation of the optimal values of h tends to an asymptotic value, which depends on the mesh size rather than on the very nature of the problem.

As expected, the plots of s_{q1} and s_{q1} (Fig. 12) show that the dispersion of the optimal values of the elastic moduli increases more than linearly with increasing δ, while a linear relationship exists between s_{q1} and s_{q1} and δ (cf. Fig. 13). The last effect can be easily explained on the basis of the linear relation between loads and displacements due to the assumption of linearly elastic behaviour.

In Fig. 13, in addition to the results of 6-, 10- and 30-measurement tests, the results of modified 10-measurement tests (black triangles) are reported. These refer to analyses based on the displacements of the points denoted by the following numbers in Fig. 1b: 1, 3, 7, 9, 10, 11, 14, 16, 18, 20.

The dispersion of the optimal values of the load par-

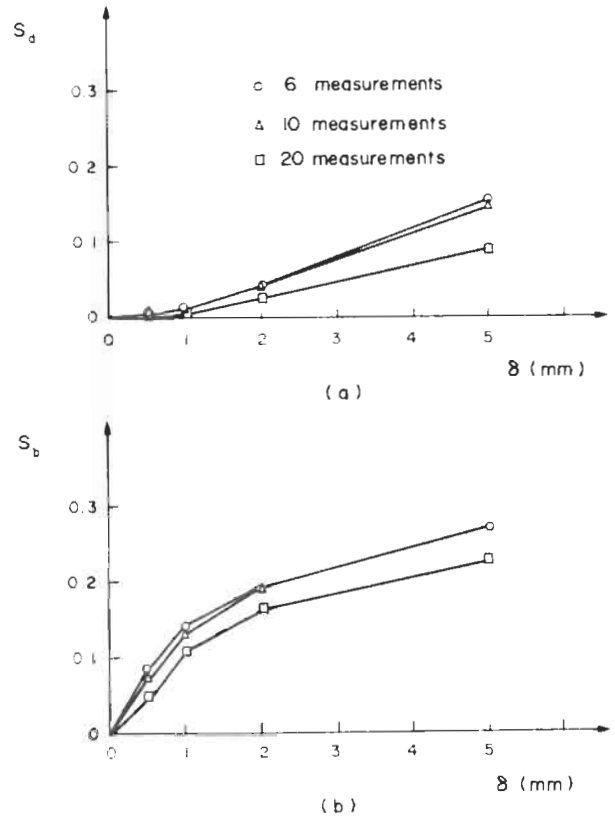

Fig. 11. Non-dimensional standard deviations s_a and s_b of the optimal values of the geometry parameters vs the input displacement approximation δ.

ameters obtained with the modified 10-measurement tests is markedly lower than that of the 10-measurement tests and practically coincides with that of the 20-measurement tests. This is due to the fact that two of the input displacements for the modified 10-measurements tests are related to points (No. 10 and 11. in Fig. 1b) very close to the points where the 'local' parameters q_1 and q_2 are defined.

Diagrams of the type shown in Figs 11–13 could be useful in designing an *in situ* test. In fact they indicate how many measurements, having a known approximation, are necessary to determine a certain unknown parameter with a prescribed accuracy. For instance, the diagrams of Fig. 12b indicate that, in order to identify the optimal values of E_2 with a non-dimensional standard deviation $s = 0.1$, it is necessary to use 6 measurements (having the pattern previously described) with approximation of ± 1 mm or 20 measurements with approximation of ± 2 mm. In engineering terms this is equivalent to saying that a given set of *in-situ* measurements, performed with an instrument of known precision, leads to a value of the unknown parameter falling within a known interval ($\pm 3s$ if a Gaussian distribution is assumed) about its 'real' value.

The same diagrams can also give useful information about the preferable locations for performing *in-situ* measurements in order to obtain an acceptable accuracy of the identifying parameters with a limited number of data.

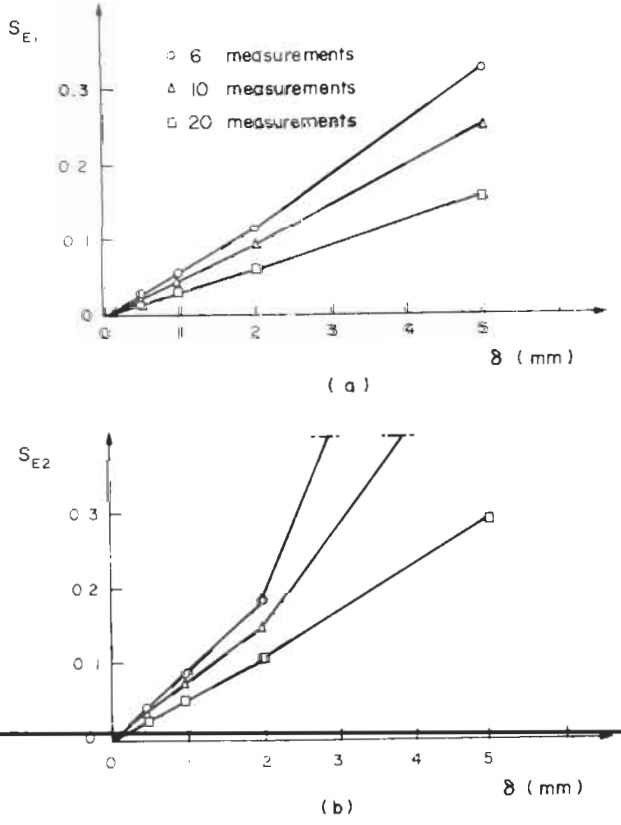

Fig. 12. Non-dimensional standard deviations s_{E1} and s_{E2} of the optimal values of the elastic moduli vs the input displacement approximation δ.

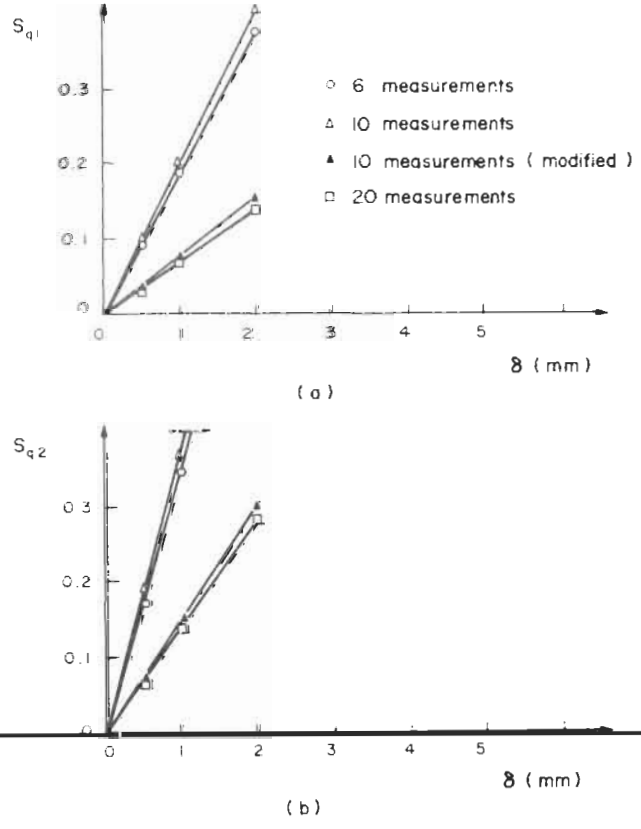

Fig. 13. Non-dimensional standard deviations s_{q1} and s_{q2} of the optimal values of the load parameters vs the input displacement approximation δ.

TABLE 1. NUMBER OF PROBLEM ANALYSES NECESSARY TO OBTAIN A NON-DIMENSIONAL STANDARD DEVIATION s_n FULFILLING EQUATION (21)

		Geometry parameters		Elastic moduli		Load parameters	
		h	d	E_1	E_2	q_1	q_2
20 Measurements	$\delta = 0.5$ mm	100	100	100	100	100	100
	$\delta = 1.0$ mm	100	100	100	100	100	200
	$\delta = 2.0$ mm	300	100	100	300	400	800
10 Measurements	$\delta = 0.5$ mm	100	100	100	100	100	300
	$\delta = 1.0$ mm	100	100	100	200	300	700
	$\delta = 2.0$ mm	300	100	100	300	600	900
6 Measurements	$\delta = 0.5$ mm	300	100	100	100	200	300
	$\delta = 1.0$ mm	400	100	200	400	500	800
	$\delta = 2.0$ mm	400	200	400	800	700	900

All the numerical tests performed for the purpose of this study are based on the solution of $N_t = 1000$ problems. However, it is likely that meaningful results could be obtained even with a smaller number of simulations. In order to assess this point, the non-dimensional standard deviation of the optimal parameters after N_t simulations, s_{N_t}, has been compared with that obtained after n simulations, s_n. In Table 1, the number of simulations is reported, for every numerical test, leading to a value of s_n fulfilling the following very severe limitation

$$|s_n - s_{N_t}| \leqslant 5\ 1000 \tag{21}$$

From the data of Table 1 it appears that, for the problem under examination, the number of analyses for most of the numerical tests could be limited to 200–400. More analyses are necessary only for some of the tests based on low quality measurements.

It has to be pointed out that the generation of the curves of Figs 11–13 requires a significant computational effort. Therefore, the use of these types of diagrams could be justified only for determining parameters of interest in Geotechnical or Rock Engineering works of particular importance (e.g. dams, underground power plants, etc.) or as an aid in improving the performance of standard *in-situ* tests of very common use (like e.g. the flat jack test).

CONCLUSIONS

In this paper some of the aspects of parameter determination problems in the field of Geomechanics have been discussed, on the basis of the numerical simulation of a hypothetical *in-situ* load test. After a brief description of *direct* and *inverse* procedures for problem solution, the discussion has been focused on the influence that the number of *in-situ* measurements (constituting the problem input data) and the experimental errors affecting them have on the results of characterization analyses. The main conclusions of the study can be summarized as follows:

(1) A relation exists between the shape of the error function associated with the parameter determination using the direct procedure, and the scatter of the optimal values of the unknown parameters in the presence of experimental errors. In particular, the higher the gradient of the error function with respect to a parameter, the lower the influence of the experimental errors on the optimal value of that parameter.

(2) The determination of 'local' parameters (e.g. values of distributed loads at some locations) appears to be more affected by the experimental errors than that of 'distributed' parameters (e.g. elastic moduli).

(3) The determination of 'local' parameters is strongly influenced by the locations where the *in-situ* measurements are performed. For instance, the value of a distributed load at a given point can be barely identified on the basis of displacement measurements performed far from the loaded zone. This is especially evident when the measurement error is a fixed quantity (e.g. ± 1 mm) and, hence, the error percentage of the measurements far from the loaded zone is likely to be much higher than that of the measurements close to it (cf. Fig. 13).

(4) For a given characterization problem it is possible to define diagrams relating the error of the parameters to be identified on the number of *in-situ* measurements, to their accuracy and to their locations. This information can be useful in order to define the minimum number and precision of the *in-situ* measurements necessary to determine values of the unknown parameters with prescribed confidence limit.

From the results of this study it appears that further research effort is desirable in the field of characterization problems in Geomechanics. A possible issue to be investigated is the relation between accuracy and number of *in-situ* measurements and error of the determined parameters, for *in-situ* tests in common use.

Acknowledgements—This paper forms part of a research project supported by the National Italian Electricity Board (ENEL), under the contract ENEL CRIS 24-78 and supervised by Professor G. Maier. The authors wish to thank Dr R. Fregonese for his helpful suggestions and stimulating comments.

Received 19 *March* 1981; *in revised form* 26 *May* 1981.

REFERENCES

1. Åmström K. J. & Eykhoff P. System identification—A survey. *Automatica* 7, 123–162 (1971).
2. Hart G. C. & Yao J. P. T. System identification in structural dynamics. *J. Engng Mech. Div. Am. Soc. civ. Engrs* 103 (EM6), 1089–1104 (1977).

3. Kavanagh K. T. Experiment versus analysis: computational techniques for the description of static material response. *Int. J. Numer. Meth. Engng* **5**, 503–515 (1973).
4. Jurina L., Maier G. & Podolak K. On model identification problems in rock mechanics. *Proc. Int. Symp. on the Geotechnics of Structurally Complex Formations*, Capri, Vol. 1, pp. 287–295 (1977).
5. Himmelblau D. M. *Applied Nonlinear Programming*. McGraw-Hill, New York (1972).
6. Gioda G. Indirect identification of the average elastic characteristics of rock masses. *Proc. Int. Conf. on Structural Foundations on Rocks*, Sydney, Vol. 1, pp. 65–73 (1980).
7. Gioda G. & Maier G. Direct search solution of an inverse problem in elastoplasticity: identification of cohesion, friction angle and *in situ* stress by pressure tunnel tests. *Int. J. Numer. Meth. Engng* **15**, 1823–1843 (1980).
8. Nelder J. A. & Mead R. A simplex method for function minimization. *Comput. J.* **7**, 308–313 (1965).
9. Maier G., Giannessi F. & Nappi A. Indirect identification of yield limits by mathematical programming. *Engng Struct.* In press (1981).
10. Maier G., Grierson D. E. & Best M. J. Mathematical programming methods for deformation analysis at plastic collapse. *Comput. Struct.* **7**, 599–612 (1977).